Applied Surface Science 257 (2011) 3336–3340

Contents lists available at ScienceDirect

Applied Surface Science

journal homepage: www.elsevier.com/locate/apsusc

Regulation of the elastic modulus of polyurethane microarrays and its influence on gecko-inspired dry adhesion

Ming Li[a,b,c], Aiwu Zhao[a,c,*], Rui Jiang[a,c], Dapeng Wang[a,c], Da Li[a,c], Hongyan Guo[a,c], Wenyu Tao[a,b,c], Zibao Gan[a,b,c], Maofeng Zhang[a,c]

[a] Institute of Intelligent Machines, Chinese Academy of Sciences, Hefei 230031, PR China
[b] Department of Chemistry, University of Science and Technology of China, Hefei 230026, Anhui, PR China
[c] State Key Laboratory of Transducer Technology, Chinese Academy of Sciences, Hefei 230031, PR China

ARTICLE INFO

Article history:
Received 20 July 2010
Received in revised form
21 September 2010
Accepted 2 November 2010
Available online 10 November 2010

Keywords:
Gecko-inspired
Dry adhesion
Polyurethane
Microarrays
Triboindenter

ABSTRACT

We studied the influence of the elastic modulus on the gecko-inspired dry adhesion by regulating the elastic modulus of bulk polyurethane combined with changing the size of microarrays. Segmented polyurethane (PU) was utilized to fabricate micro arrays by the porous polydimethyl siloxane (PDMS) membrane molding method. The properties of the micro arrays, such as the elastic modulus and adhesion, were investigated by Triboindenter. The study demonstrates that bulk surfaces show the highest elastic modulus, with similar values at around 175 MPa and decreasing the arrays radius causes a significant decrease in *E*, down to 0.62 MPa. The corresponding adhesion experiments show that decrease of the elastic modulus can enhance the adhesion which is consistent with the recent theoretical models.

© 2010 Elsevier B.V. All rights reserved.

1. Introduction

The climbing ability of geckos is attributed to fibrillar arrays, consisting of stiff, hydrophobic β-keratin which covers the bottom of gecko's feet. Such high dry adhesion between the feet and surfaces originates from Vander Waals forces [1–3]. Dry adhesion which is clean and environment-friendly, can be applied to biomedical patch [4] and climbing robot [5,6]. As a consequence, increased effort has been paid recently to mimic gecko's feet by using polymer arrays structures [7]. Fabrication techniques such as electron-beam lithography, photolithography, etching techniques and polymer molding techniques were utilized for fabricating pillar structures [8,9]. To mimic gecko foot hairs, surface design parameters such as pillar size, shape, elastic modulus, or tilt angle need to be considered [10–15]. In particular, Autumn et al. [16] found that the effective modulus of a gecko setal adhesion is much lower than that of bulk β-keratin and decrease of effective modulus can enhance the adhesion. Maybe it is such combination of "hardness" and "softness" that realize the high dry adhesion. Up to now, the influence of the elastic modulus on dry adhesion has seldom been studied experimentally, although recent theoretical models [17,18] predict the importance of the elastic modulus in dry adhesion. Following this concept, we try to utilize a material whose elastic modulus can be tuned easily to realize the modulation of the dry adhesion. As we know, segmented polyurethanes consisting of hard segments (HS) and soft segments (SS) can be obtained easily, which makes them useful in some applications such as adhesives and biomedical materials [19]. The mechanical properties of segmented polyurethanes, such as elastic modulus are highly dependent on the HS/SS ratio and the phase separation [20,21].

In this paper, we fabricated a series of segmented PU from 4,4′-diphenylmethane diisocyanate (MDI), polyoxytertramethylene glycol (PTMG) (Mn = 1000), with 1,4-butanediol (BDO) as the chain extender. Microarrays patterned surfaces with different radius were obtained by the porous polydimethyl siloxane membrane molding method. By varying the ratios of hard and soft segments of the bulk PU and changing the radius of the PU arrays, regulation of the elastic modulus of PU micro arrays is achieved. The influence of these parameters on the adhesion properties of the surface is described and compared with theoretical predictions. To measure the adhesion properties of the arrays, such as elastic modulus and adhesion, Triboindenter was utilized.

* Corresponding author at: Institute of Intelligent Machines, Chinese Academy of Sciences, Hefei 230031, PR China. Tel.: +86 551 5593360; fax: +86 551 5592420.
E-mail address: awzhao@iim.ac.cn (A. Zhao).

0169-4332/$ – see front matter © 2010 Elsevier B.V. All rights reserved.
doi:10.1016/j.apsusc.2010.11.017

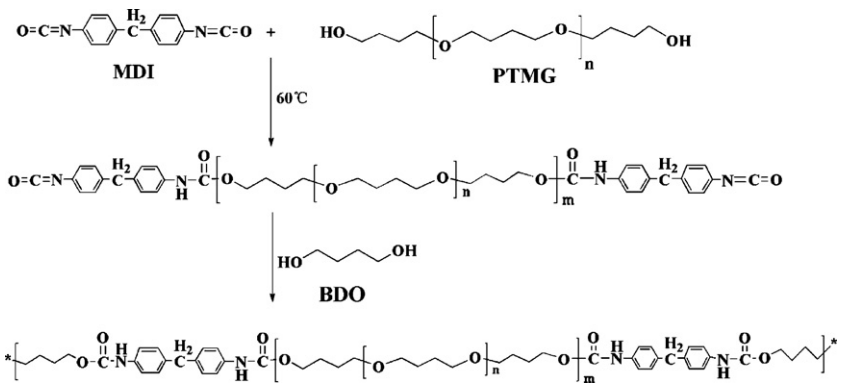

Fig. 1. Elementary steps for the synthesis of polyurethane.

2. Experimental

2.1. Chemicals

MDI and PTMG were purchased from Mitsubishi Chemical. BDO was purchased from Chemical Co. Sylgard 184 was purchased from Dow Corning (MI, USA). BDO and PTMG were dried at 80 °C under vacuum overnight to ensure the removal of water that may interfere with the isocyanate reactions. Dimethylformamide (DMF) was dried over $MgSO_4$. All the reagents used in this work were of analytical grade.

2.2. Synthesis of polyurethane

The preparation procedure of PU is shown in Fig. 1. MDI was placed into a four-necked beaker equipped with dropping funnel, mechanical stirrer, heating oil bath, Ar inlet and outlet. The temperature of the oil bath was increased to 60 °C. Then PTMG was added dropwise into beaker through dropping funnel. It took almost 1.0 h to obtain NCO terminated prepolymer. The resulting viscous solution was diluted with 10 ml of DMF. Conversion of the prepolymer into the final PU was carried out by stirring the prepolymer vigorously, and then adding chain extender, BDO. The resulting polymer was cast into a PDMS plate to form a uniform sheet of 2–3 mm thickness. The synthesized polymer was then placed in a hot air circulating oven at 100 °C and cured overnight.

2.3. Fabrication of gecko-mimic hair arrays

We obtained microarrays by pouring variable synthetic polyurethane over the PDMS template in a vacuum chamber which

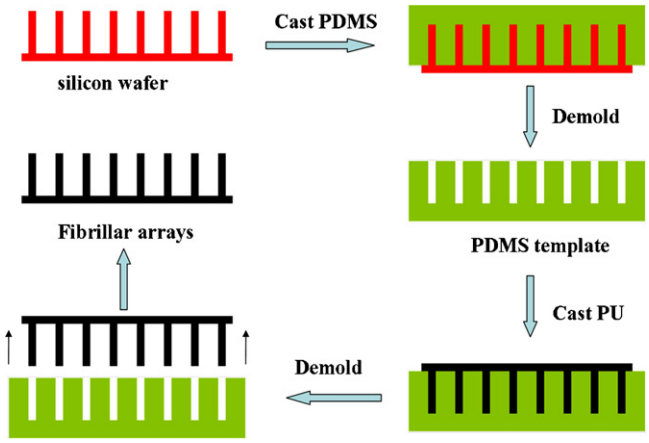

Fig. 2. Fabrication process of gecko-mimic microarrays.

is depicted in Fig. 2. PU microarrays can be peeled off from PDMS easily due to hydrophobicity and thermodynamic stability of the PDMS. The first step was to create a positive mold for the hairs by a patterned silicon wafer. The silicon micro cylindrical fiber arrays were fabricated by inductively coupled plasma (ICP) etching process. In the second step, PDMS was poured over the mold and then solidified at 70 °C for 4 h in the oven. After peeling off from the silicon mechanically, the PDMS template with microhole arrays was obtained. Shown in Fig. 3 are the scanning electron microscopy images for one of the microarrays with 7 μm diameter 50 μm length and 5 μm spacing between each array. Therefore, microarray with high-aspect-ratio can be achieved.

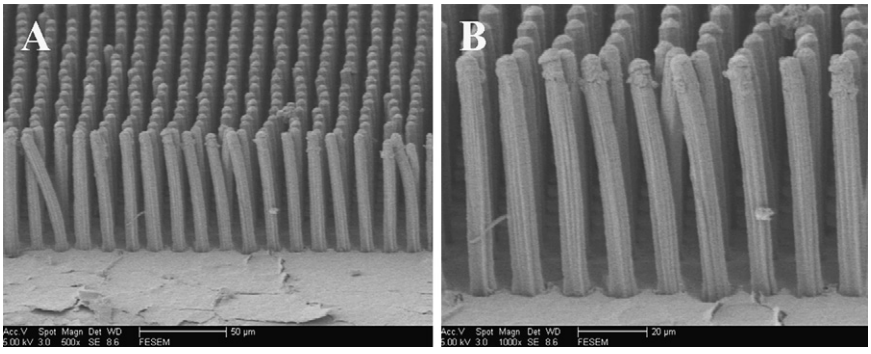

Fig. 3. Scanning electron microscopy image of fabricated polyurethane microarrays: (A) microarrays with 7 μm diameter 50 μm length and 5 μm spacing between each array; (B) an enlarged view of A.

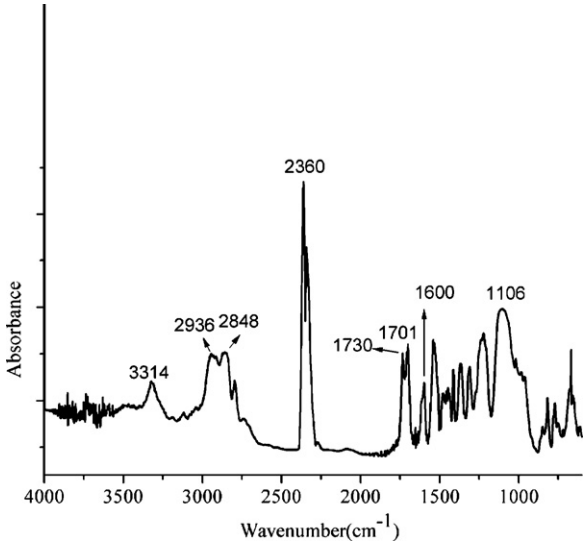

Fig. 4. FTIR spectrum of synthesized polyurethane.

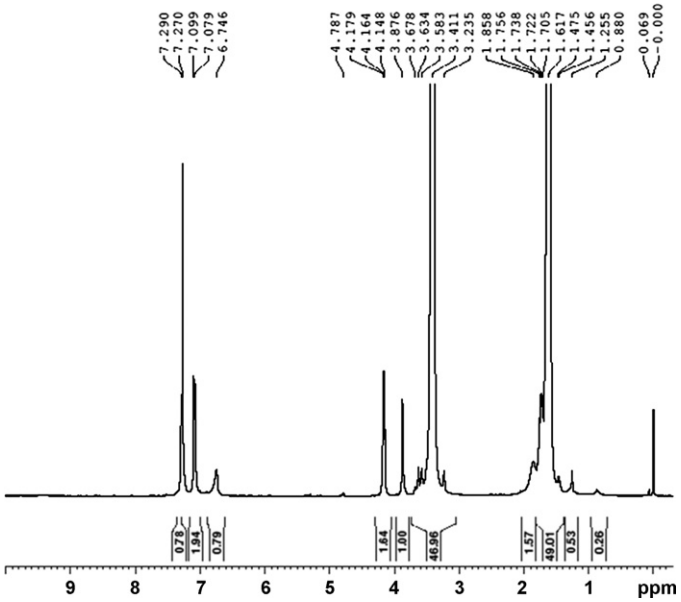

Fig. 5. ^{1}H NMR spectrum of synthesized polyurethane.

3. Results and discussion

3.1. IR characterization of synthesized PU

Infrared spectrum was obtained on a Thermo-Fisher Nicolet is Fourier transform infrared spectrometer (FTIR). Fig. 4 displays the FTIR spectrum of fabricated polyurethane. There are characteristic peaks of N–H (3314 cm^{-1}) and C=O (1701–1730 cm^{-1}). C–H aliphatic stretches bands (2936, 2848 cm^{-1}) are also observed. The absorption band at 1106 cm^{-1} originates from C–O–C group. There are phenyl C–H absorption bands at 1600 cm^{-1}. The disappearance of the absorption bands of the NCO group (2270 cm^{-1}) of MDI also proves the synthesis of the polyurethane.

3.2. ^{1}H NMR characterization of synthesized PU

^{1}H NMR spectrum of PU was run at 400 MHz on a Bruker AVANCE AVIII 400 with the sample dissolved in $CDCl_3$ in a 5 mm tube with tetramethylsilane (TMS) as internal standard. It is evident from Fig. 5 that the peak appears at 6.746 ppm, which is assigned to the protons of –CONH–. Two peaks at 7.290 and 7.079 ppm are relative to the benzene protons, and the peak appears at 3.411 deals with $–CH_2O–$ protons of PTMG and 4.179 ppm originates from polyether–urethane $–COOCH_2–$. Besides, the peaks at 3.876 ppm assigned to the protons of BDO adjacent to oxygen atom, the peaks at 1.617 ppm corresponding to the $–CH_2CH_2–$ protons of PTMG and BDO.

3.3. The elastic modulus and adhesion

The elastic modulus and adhesion of PU materials were measured by Triboindenter (Hysitron, Inc., Minneapolis, USA). The nanoindenter was operated in displacement control to obtain the curves of the load versus displacement. The selected probe was Berkovich tip (1 μm × 100 μm). Indenter loading resolution ratio < 1 nN and displacement resolution < 0.04 nm. Tests were repeated six times on each PU sample to obtain the mean data. The sample was placed on the positioning stage, and the probe was brought in contact. After compressive preloading, the probe was retracted. The maximum vertical displacement of the probe was 200 nm, and the positioning accuracy was 1 nm. Tests were repeated six times on each PU sample and obtained the mean data. The elastic modulus was calculated from the unloading curves by Oliver–Pharr method [22]. The typical loading–unloading curves of PU sample are illustrated in Fig. 6. Solid and broken arrows indicate linear fits for loading and unloading, respectively. Force versus displacement of microarrays loaded and unloaded vertically. The elastic modulus of bulk PU is then analyzed according to the equation:

$$S = \left.\frac{dp}{dh}\right|_{h=h_m} = \frac{2}{\sqrt{\pi}} E\sqrt{A}$$

where $S = dP/dh$ is the experimentally measured stiffness of the unloading data. E is the elastic modulus, and A is the contact area evaluated at h_m the area of the elastic contact. For the microarrays patterned surfaces, the effective elastic modulus can be calculated from Hookean elasticity model as following:

$$\sigma = \frac{P}{A}; \quad \varepsilon = \frac{h}{L}; \quad E = \frac{d\sigma}{d\varepsilon} = \frac{L}{A}\frac{dP}{dh}$$

where P is the applied load. A is the contact area and L is array height and h is change in array height in response to this force. Based these methods, We can clearly see from Fig. 7 that for the PU with the same composition, bulk surfaces show the highest elastic modulus, with similar values at around 175 MPa and decreasing the arrays radius causes a significant decrease in E, down to 0.62 MPa. We

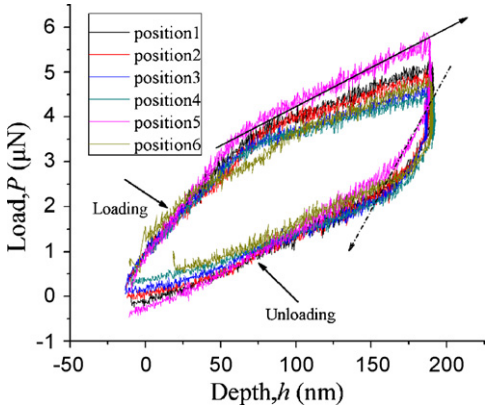

Fig. 6. Loading–unloading curves of bulk polyurethane sample. Solid and broken arrows indicate linear fits for loading and unloading, respectively.

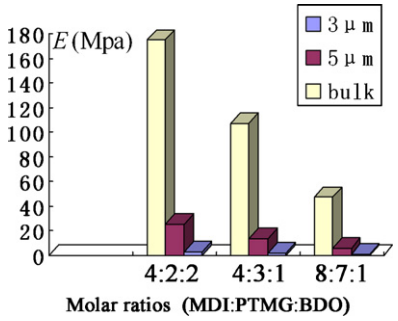

Fig. 7. Decrease of the elastic modulus versus composition and surface feature.

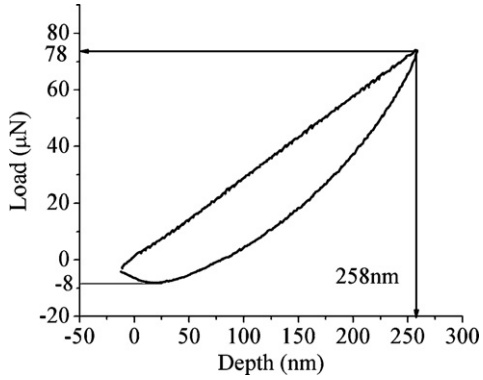

Fig. 8. Nanoindenter adhesion test results for a microarrays structure indented with three-side pyramid-type Berkovich tip.

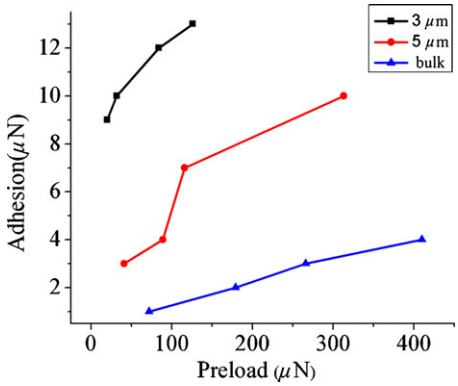

Fig. 9. Enhancement of the adhesion versus the preload.

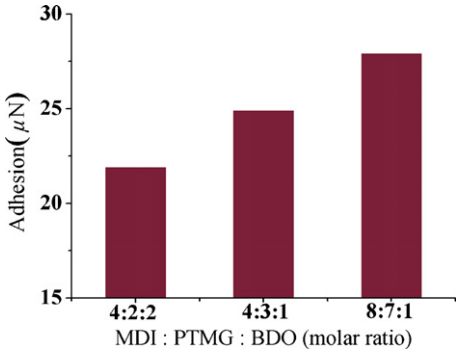

Fig. 10. Enhancement of the adhesion measured on the polyurethane patterned with 3-μm-diameter microarrays versus the composition of polyurethane.

can also see that for the microarrays with the same size diameter, decreasing the ratios of MDI and PTMG causes a significant decrease in *E*. This means that, by varying the composition of segmented polyurethanes, elastic modulus decreases when the percentage of soft segment increases. The hard segments of PU have urethane group, i.e. –NHCOO– and the soft segments of PU have the ester group, i.e. –COO–. By varying the ratios of hard and soft segments of the bulk PU and changing the radius of the PU arrays, regulation of the elastic modulus of PU micro arrays can be achieved easily. Hereby, we successfully realize the regulation of the elastic modulus by changing the size of microarrays of patterned surfaces and varying the ratios of hard and soft segments of the PU.

To determine the adhesion, Operating in displacement control, load versus displacement data were collected from the nanoindenter and analyzed to determine the adhesion. The sample was placed on the positioning stage, and the probe was brought in contact. After compressive preloading, the probe was retracted. The maximum vertical displacement of the probe was 200 nm, and the positioning accuracy was 1 nm. Indenter loading resolution ratio < 1 nN and displacement resolution < 0.04 nm. Adhering surfaces would produce a distinctive pull-off behavior, where the unloading curve would make a sudden jump (Fig. 8). In the case of an adhesion event the number is negative, taken to be the maximum adhesion. Based on this, from Fig. 9 we can clearly see that, for the polyurethane with the same composition, microarrays patterned surfaces with decreasing pillar radius showed higher adhesion at any preload. 3-μm-diameter arrays hold higher adhesion force than that of 5-μm-diameter arrays. The size effect of adhesion can be analyzed by Johnson–Kendall–Roberts (JKR) theory [23]:

$$\sigma = \frac{P}{\pi a^2} = \left(\frac{3\Delta\gamma E^2}{2\pi^2 R}\right)^{1/3}$$

where $\Delta\gamma$ is work of adhesion, E the elastic modulus, R radius. So the adhesion σ is inversely proportional to the one-third power of the equivalent radius. Thus, the adhesion increases when radius

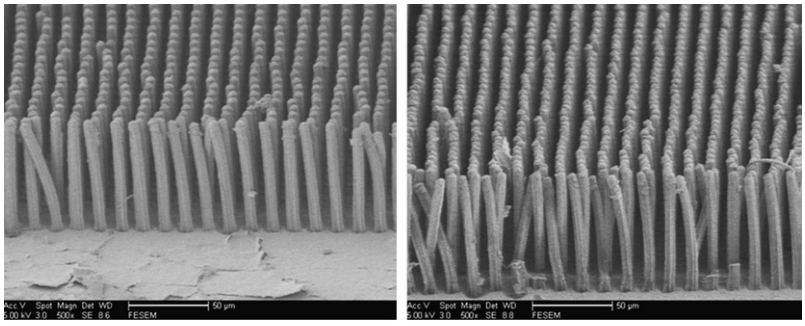

Fig. 11. The contrastive SEM images of foot-hair before detection and after detection.

decreases, which is consistent with the adhesion test results. In addition, it is obviously from Fig. 10 that, for the same size arrays patterned surface, by varying the composition of segmented polyurethanes, the adhesion increases when the percentage of soft segment increases. As mentioned in the elastic modulus tests, for microarrays with the same size, decreasing the ratios of MDI and PTMG causes a significant decrease in E. These adhesion test results are consistent with the results of the elastic modulus that decrease of the elastic modulus can enhance the adhesion. The data for all samples were found to be reproducible and no much collapse and twist was observed because the theoretical buckling criterion [24] predicts a minimum compressive load required for buckling (41 mN), which is well above our maximum preload (6 μN). For this reason, buckling events can be neglected in our experiments. Fig. 11 is the contrastive SEM images of foot-hair before detection and after detection.

4. Conclusions

In this study, we have achieved to regulate the adhesion of PU micro arrays by varying the ratio between MDI and PTMG combined with changing the size of micro arrays. The results show that bulk surfaces show the highest effective modulus, with similar values at around 175 MPa and decreasing the arrays radius causes a significant decrease in E, down to 0.62 MPa. For the same surface features, decrease of the ratios of MDI and PTMG causes a decrease in E. For the PU with the same composition, the micro arrays patterned surfaces with decreasing pillar radius showed higher adhesion than of bulk smooth PU at any preload. 3-μm-diameter arrays hold higher adhesion force than that of 5-μm-diameter arrays. For the same size arrays patterned surface, the adhesion increases when the percentage of soft segment increases. It is consistent with theoretical model that decrease of effective modulus can enhance the adhesion.

Acknowledgments

This work was supported by National Basic Research Program of China (2011CB302103) and Natural Science Foundation of China (No. 20873153). We also thank the State Key Laboratories of Transducer Technology for financial support.

References

[1] A.P. Russell, J. Zool. Lond. 176 (1975) 437.
[2] K. Autumn, L.A. Liang, S.T. Hsieh, W. Zesch, T.W. Kenny, R. Fearing, R.J. Full, Nature 405 (2000) 681.
[3] K. Autumn, M. Sitti, A. Peattie, A. Hansen, R.J. Full, Proc. Natl. Acad. Sci. U. S. A. 99 (2002) 12252.
[4] A. Mahdavi, L. Ferreira, C. Sundback, J.W. Nichol, E.P. Chan, Proc. Natl. Acad. Sci. U. S. A. 105 (2008) 2307.
[5] M.P. Murphy, M. Sitti, IEEE-ASME Trans. Mechatron. 12 (2007) 330.
[6] D. Santos, M. Spenko, A. Parness, S. Kim, M. Cutkosky, J. Adhes. Sci. Technol. 21 (2007) 1317.
[7] A.K. Geim, S.V. Dubonos, I.V. Grigorieva, K.S. Novoselov, A.A. Zhukov, S.Y. Shapoval, Nat. Mater. 2 (2003) 461.
[8] M. Sitti, R.S. Fearing, J. Adhes. Sci. Technol. 17 (2003) 1055.
[9] H.E. Jeong, J.K. Lee, H.N. Kim, S.H. Moon, K.Y. Suh, Proc. Natl. Acad. Sci. U. S. A. 106 (2009) 5639.
[10] A. Del Campo, C. Greiner, E. Arzt, Langmuir 23 (2007) 10235.
[11] C. Greiner, A. Del Campo, E. Arzt, Langmuir 23 (2007) 3495.
[12] S. Kim, M. Sitti, Appl. Phys. Lett. 89 (2006) 261911.
[13] S. Kim, M. Sitti, C.Y. Hui, R. Long, A. Jagota, Appl. Phys. Lett. 91 (2007) 161905.
[14] B. Aksak, M.P. Murphy, M. Sitti, Langmuir 23 (2007) 3322.
[15] E.P. Chan, C. Greiner, E. Arzt, A.J. Crosby, MRS Bull. 32 (2007) 496.
[16] K. Autumn, C. Majidi, R.E. Groff, A. Dittmore, R. Fearing, J. Exp. Biol. 209 (2006) 3558.
[17] B.N.J. Persson, S.J. Gorb, Chem. Phys. 119 (2003) 11437.
[18] B.N.J. Persson, J. Chem. Phys. 118 (2003) 7614.
[19] R.W. Seymour, G.M. Estes, S.L. Cooper, Macromolecules 3 (1970) 579.
[20] C.M. Brunette, S.L. Hsu, W.J. MacKnight, Macromolecules 15 (1982) 71.
[21] M. Barikani, M. Mohammadi, Carbohydr. Polym. 68 (2007) 773.
[22] G.M. Pharr, A. Bolshakav, J. Mater. Res. 17 (10) (2002) 2600.
[23] K.L. Johnson, K. Kendall, A.D. Roberts, Proc. R. Soc. Lond. Ser. A 324 (1971) 301.
[24] C.Y. Hui, A. Jagota, Y.Y. Lin, E.J. Kramer, Langmuir 18 (4) (2002) 1394.